A 2D/1D algorithm for effective cross sections generation in fast reactor neutronic transport calculations

B. Faure, P. Archier, J.-F. Vidal, L. Buiron

A 2D/1D algorithm for effective cross sections generation in fast reactor neutronic transport calculations

Bastien Faure,[a,*] Pascal Archier,[a] Jean-François Vidal,[a] and Laurent Buiron[a]

[a] *CEA, DEN, DER, SPRC*
Cadarache, F-13108, Saint-Paul-lez-Durance, France
[*]Email: bastien.faure@cea.fr

Number of pages: 25

Number of tables: 3

Number of figures: 3

Abstract

Fast resolution of the Boltzmann transport equation over a nuclear reactor core presupposes the definition of homogenized and energy collapsed cross sections. In modern sodium fast reactors that rely on heterogeneous core designs, anisotropy in the neutrons propagation cannot be neglected so three-dimensional models should be preferred to compute those effective cross sections. In this paper, the 2D/1D approximation is used to avoid computationally expensive 3D calculations while preserving consistent angular representations of the neutron flux. An iterative procedure is defined to solve the 2D/1D equations and produce coarse group homogenized cross sections that account for 3D transport effects. Accuracy of the algorithm is tested on a realistic model of the ASTRID core showing very good results against Monte Carlo simulations for all neutronic parameters (eigenvalue, sodium void worth and fission map distribution).

Keywords — Neutronics, Transport, 2D/1D method, Homogenization, Energy condensation, Sodium Fast Reactor

I. INTRODUCTION

Next generation of nuclear reactors is asked to meet very high safety criteria in order to prevent as much risk of accident as possible. In the field of neutronics, reaching those standards presupposes the demonstration of a good understanding of the physical processes that take place in the reactor core. Given the progress that has been made in computer science, numerical simulation nowadays provides an efficient tool to perform such a demonstration and is therefore widely used.

Consequently, the research community has concentrated many efforts in providing detailed and precise solutions to three-dimensional whole-core transport problems. While taking a significant step forward in the quest for accuracy, those efforts also showed that obtaining such solutions often required long hours of calculation over large-scale parallel systems with hundreds and even thousands of processors. As a result, they are not well adapted to the current industry's needs which demand a large number of calculations in a limited amount of time and with limited computer resources [1]. For practical application then, we may assess with confidence that full core calculations will still be performed for some time over coarse spatial and energy meshes. They will therefore rely on homogenized multigroup *effective cross sections*.

Those effective parameters are classically obtained from two-dimensional *lattice* calculations in which neutron fluxes are computed over axially infinite and radially periodic assembly patterns and used to weight the input cross sections. Taking advantage of nearly periodic core designs, limited axial heterogeneities and neutron' small mean free paths, the lattice paradigm has proven its efficiency for pressurized water reactors (PWR) applications.

On the contrary, current tendency for modern sodium-cooled fast reactors (SFR) is to present strong axial heterogeneities. While allowing a significant reduction of the reactivity void worth compared to homogeneous designs, this feature however questions the validity of the above mentioned procedure for cross sections generation. In particular, the quite large mean free paths of neutrons in sodium-cooled technologies gives birth to particle exchanges between distinct axial layers and therefore produces spectrum shifts along the vertical axis and anisotropic structures in the neutron flux.

More precisely, it has been shown in a previous work [2] that large errors could indeed be found when two-dimensional lattice parameters were used to compute neutron fluxes over axially heterogeneous SFR cores such as the French CFV (*coeur a faible vidange* or low sodium void effect

core) prototype ASTRID. The conclusion of the analysis was that infinite lattice calculations were unable to yield consistent effective cross sections because they neglect axial modes of the angular flux. Moreover, it was proven that biases could be significantly reduced if such modes were incorporated in the calculation and used in the cross sections weighting process.

A straightforward way to access full angular modes of the flux that are representative of the core situation is the application of the method of characteristics (MOC) to three-dimensional transport problems [3]. However, considerable efforts are needed to solve the 3D MOC equations, making its use rather inappropriate in the scope of cross sections generation were fluxes are used only as weight functions.

In this paper, consistent information for cross sections generation is retrieved from a 2D/1D approximation to the 3D transport equation. Based upon the original *2D/1D fusion method* [4], its basic idea is to couple several two-dimensional lattice calculations through axial leakage computed over one-dimensional models. Taking advantage of the angular information that is contained in the axial leakage, it is shown that three-dimensional transport effects can be successfully stored in effective cross sections.

The aim of the paper is to present this 2D/1D cross sections weighting algorithm and to stress its accuracy in realistic situations. Its organization is as follows: Sec. II addresses the theory of effective cross sections generation while Sec. III presents the 2D/1D algorithm together with its practical implementation in the APOLLO3® code [5]. In Sec. IV, numerical results are presented and discussed. The paper ends with a general conclusion and perspectives for future work.

II. EFFECTIVE CROSS SECTIONS GENERATION

In this section, the transport equation is introduced and the theory of cross sections averaging is discussed.

II.A. The transport equation

The steady state Boltzmann transport equation for the neutron flux ψ reads

$$\left(\vec{\Omega}\cdot\vec{\nabla}+\Sigma\right)\psi = q \tag{1}$$

where Σ is the total macroscopic cross section and q a source term. Equation (1) stands in a geometrical domain D, for all neutron directions and at all energies (i.e. $(\vec{r}, E, \vec{\Omega}) \in D \times \mathbb{R}^+ \times S_{4\pi}$) provided that the incoming neutron density at the boundary is known (i.e. $\psi = \psi_{in}$ for $(\vec{r}, \vec{\Omega}) \in \partial D \times S^-_{2\pi}$).

In a reactor core, fission and scattering reactions are the main contributors to the neutron source. Introducing the scattering H and production F operators q reads

$$q = \left(H + \frac{1}{k} F \right) \psi \tag{2}$$

In that case, equation (1) is casted in the form of an eigenvalue problem. Assuming k is the largest positive eigenvalue, the eigen-pair (k, ψ) is called *fundamental mode*. It is the solution that is handled by most numerical methods and the one we are interested in.

For practical applications, the energy interval is split into N_g bins $\mathbb{R}^+ = \bigcup_g [\![E_g; E_{g+1}]\!]$ and continuous energy data are replaced by their group averaged value. Flux ψ is sought under the form of a vector $\psi = (\psi^g)_{g \in [\![1; N_g]\!]}$.

In this well known multigroup formalism, the scattering operator H is written in terms of the Legendre moments of the scattering cross section $(\Sigma_{s,l}^{g' \to g})_{l \in \mathbb{N}}$ as

$$H\psi^g(\vec{r}, \vec{\Omega}) = \sum_{g'=1}^{N_g} \sum_{l=0}^{+\infty} \frac{2l+1}{4\pi} \Sigma_{s,l}^{g' \to g}(\vec{r}) \sum_{m=-l}^{+l} \phi_{lm}^{g'}(\vec{r}) R_{lm}(\vec{\Omega}) \tag{3}$$

The production operator F is also developed in terms of a production cross section $\nu\Sigma_f^{g' \to g}$ as

$$F\psi^g(\vec{r}, \vec{\Omega}) = \frac{1}{4\pi} \sum_{g'=1}^{N_g} \nu\Sigma_f^{g' \to g}(\vec{r}) \phi_{00}^{g'}(\vec{r}) \tag{4}$$

Here $\nu\Sigma_f^{g' \to g}$ is a non-standard but compact notation that will be used throughout this paper for the sake of simplicity. It stands for the sum over fissile isotopes of the product of fission spectra χ times multiplicity ν times fission cross section Σ_f.

Real spherical harmonics $(R_{lm})_{m \in [\![-l; l]\!]}^{l \in \mathbb{N}}$ have also been used as a projection basis for angular dependent functions. Angular flux moments are defined as

$$\phi_{lm}^g(\vec{r}) = \int_{S_{4\pi}} d^2\Omega \; \psi^g(\vec{r}, \vec{\Omega}) R_{lm}(\vec{\Omega}) \tag{5}$$

II.B. Cross sections averaging

A typical SFR fuel assembly is composed of 250 fuel pins requiring thus at least 600 radial volumes to discretize fuel, clad, coolant and internal structures. Considering that there are approximately 500 assemblies in the core and that 100 distinct axial layers are required to catch the axial variations of the flux, a total of 30 million spatial volumes is a minimum. If we also suppose that 250 angles are required for the $\vec{\Omega}$ variable and that $N_g = 2000$ is a realistic number of energy groups (when resonances are accounted for with a self-shielding formalism), we get the digit of 1.5 10^{13} unknowns for the flux. Assuming a simple precision floating-point storage, the latter represents a total of 60 terabytes of memory to which must be appended the weight of additional data such as cross sections, geometry description or transport acceleration factors.

Given that such a huge amount of computer resources is not suited for industrial applications, cross sections averaging is required to reduce the number of energy groups (energy condensation) and spatial mesh cells (homogenization) in whole core calculations. Its basic idea is to preserve reaction and leakage rates between detailed and coarse models of the same transport problem.

In order to derive analytical expressions for effective cross sections, we first introduce compact notations for spatial integration and group summation

$$< f^g >_{iG} = \int_{D_i} d^3r \sum_{g \in G} f^g(\vec{r}, \vec{\Omega}) \tag{6}$$

$$< f^{g' \to g} >_{iG'G} = \int_{D_i} d^3r \sum_{g' \in G'} \sum_{g \in G} f^{g' \to g}(\vec{r}, \vec{\Omega}) \tag{7}$$

where $D_i \subset D$ is a generic sub-domain and $G = \{g_1, \ldots, g_p\}$, $G' = \{g_{1'}, \ldots, g_{p'}\}$ are energy group indexes sets. We then define the following quantities

$$\Sigma_i^G(\vec{\Omega}) = \frac{< \Sigma^g \psi^g >_{iG}}{< \psi^g >_{iG}} \tag{8}$$

$$\Sigma_{s,lm,i}^{G' \to G} = \frac{< \Sigma_{s,l}^{g' \to g} \phi_{lm}^{g'} >_{iG'G}}{< \phi_{lm}^{g'} >_{iG'}} \tag{9}$$

$$\nu\Sigma_{f,i}^{G' \to G} = \frac{< \nu\Sigma_f^{g' \to g} \phi_{00}^{g'} >_{iG'G}}{< \phi_{00}^{g'} >_{iG'}} \tag{10}$$

At first sight, such definitions are good candidates for effective total, scattering and production cross sections. They however suffer from two well known limitations that are here recalled:

1. They generally do not preserve exactly the neutronics balance because $< \psi^g >_{iG}$ differs from the integral of the coarse-mesh transport solution. Two exceptions might be found, when only energy collapsing is considered [6] or when a whole space homogenization is performed with zero net leakage boundary conditions [7]. In all other cases, preservation of leakage rates is not guaranteed.

2. Averaging equation (8) with the angle dependent function ψ introduces anisotropy in the total cross section. As a result, Σ_i^G does not define a transport equation over an isotropic medium and is thus not compatible with most neutron transport codes. Similarly, the dependence of the scattering cross section with azimuthal index m in equation (9) is not standard.

To address the first issue, SPH factors have been proposed in the past by Hebert [8] for partial homogenization and pin-by-pin power reconstruction. In the same time, Smith also introduced current (and latter flux) discontinuity factors [9] to deal with general boundary conditions (black box homogenization).

As for the second point, a standard solution is the *flux-volume* collapsing technique that consists in replacing angular dependent weights ψ and ϕ_{lm} by the isotropic scalar flux ϕ_{00}. If this approximation clearly implies the loss of any angular information, consistency can be recovered in the framework of diffusion theory because diffusion coefficients can be constructed in such a way as to preserve linearly anisotropic transport effects. When transport theory is used for whole core calculations however, high order angular effects should be stored in effective cross sections.

In the generalized energy condensation theory introduced by Rahnema and co-workers [10, 11], the angular dependence of the total cross section is shifted into a variation term and transferred to the right hand side of the transport equation. Following the same idea, Vidal incorporated this variation term into the within group scattering rate [6, 12] and used a least-square minimization technique to define a conventional scattering cross section.

In this paper, we will follow this latter approach and take the following definitions for effective total and l-th order scattering cross sections:

$$\Sigma_i^G = \frac{< \Sigma^g \phi_{00}^g >_{iG}}{< \phi_{00}^g >_{iG}} \tag{11}$$

$$\Sigma_{s,l,i}^{G'\to G} = \frac{\sum_{m=-l}^{+l} \Sigma_{s,lm,i}^{G'\to G} \left(< \phi_{lm}^{g'} >_{iG'} \right)^2}{\sum_{m=-l}^{+l} \left(< \phi_{lm}^{g'} >_{iG'} \right)^2} + \delta_{G,G'} \left(\Sigma_i^G - \Sigma_{l,i}^G \right) \tag{12}$$

where $\delta_{G,G'}$ is the Kronecker delta, $\Sigma_{s,lm,i}^{G'\to G}$ is taken from equation (9) and $\Sigma_{l,i}^G$ reads

$$\Sigma_{l,i}^G = \frac{\sum_{m=-l}^{+l} < \phi_{lm}^g >_{iG} < \Sigma^g \phi_{lm}^g >_{iG}}{\sum_{m=-l}^{+l} \left(< \phi_{lm}^g >_{iG} \right)^2} \tag{13}$$

Equation (10) defines a standard cross section and is therefore used for the production probability.

In the following, the combination of equations (10), (11) and (12) will be referred to as *flux moments weighting*. It allows a better conservation of anisotropic transport effects and is therefore expected to improve the standard (scalar) flux-volume weighting technique.

III. THE 2D/1D METHOD FOR CROSS SECTIONS GENERATION

The *2D/1D* terminology refers to a class of computational methods that proposes to solve the three-dimensional Boltzmann transport equation by resorting to transverse integration in order to reduce the phase-space dimensions. In this section, we present how the 2D/1D method can be used in the scope of effective cross sections generation.

The original idea comes from Cho and colleagues that developed a *fusion* method for the CRX code coupling two-dimensional radial MOC calculations one to another through axial leakage retrieved from one-dimensional S_N solutions [4]. At the same time, a similar method was also implemented in the DeCART code by another group of researchers that proposed to embed the axial leakage calculation into three-dimensional coarse mesh finite difference simulations [13].

In the past few years, a growing interest was found all around the world for the 2D/1D method [14, 15]. In particular, a mathematical analysis of the 2D/1D equations and their numerical counter part was provided by the MPACT development team [16] and some of the main limitations, such as the negative source issue, were recently lifted [17].

A particular feature of the 2D/1D method is that it requires a homogenization procedure

to produce the one-dimensional calculation mesh and a *de-homogenization* method to build radial shapes for axial leakage. In order to get rid of those approximations, some authors proposed to equalize the number of axial calculations to the number of two-dimensional radial cells [18]. However, it is our opinion that computational advantages can be taken from the homogenization step so this latter approach will not be considered in this paper.

In the following, the basic theory of the 2D/1D method is presented and choices made for their practical implementation in the APOLLO3® code are discussed.

III.A. General equations

The starting point is the 3D transport equation (1) whose solution is written (k, ψ). For the sake of clarity, energy group indexes are dropped out in this section.

The geometrical domain D is partitioned into axial Z_i and radial D_r sub-domains such as $D = \bigcup_i Z_i \times \bigcup_r D_r$. The axial partition is chosen so that cross sections are axially invariant in a given layer Z_i i.e.

$$\forall z \in Z_i, \quad \Sigma(\vec{r}) = \Sigma(x, y) \tag{14}$$

Equation (1) is then successively integrated axially over Z_i and radially over D_r yielding the following set of equations

$$\left(\vec{\Omega} \cdot \vec{\nabla}_{xy} + \Sigma\right) \psi_i = q_i - L_i \tag{15}$$

$$\left(\mu \partial_z + \Sigma_r\right) \psi_r = q_r - L_r \tag{16}$$

where ψ_i, ψ_r are integrated fluxes

$$\psi_i(x, y, \vec{\Omega}) = \int_{Z_i} dz \; \psi(\vec{r}, \vec{\Omega}) \tag{17}$$

$$\psi_r(z, \vec{\Omega}) = \int_{D_r} dxdy \; \psi(\vec{r}, \vec{\Omega}) \tag{18}$$

and L_i, L_r transverse leakage

$$L_i(x, y, \vec{\Omega}) = \mu \int_{Z_i} dz \; \partial_z \psi(\vec{r}, \vec{\Omega}) \tag{19}$$

$$L_r(z,\vec{\Omega}) = \int_{D_r} dxdy\ \vec{\Omega}\cdot\vec{\nabla}_{xy}\psi(\vec{r},\vec{\Omega}) \tag{20}$$

∂_z symbolizes the partial derivative towards z and μ is the polar cosine.

Applying operators H and F of equation (2) to flux ψ_i (resp. ψ_r), one finds the analytical expression for source q_i (resp. q_r). Cross section Σ is the one from the original 3D problem because of assumption (14). On the contrary, the definition of Σ_r requires a 3D flux homogenization

$$\Sigma_r = \frac{<\Sigma\psi>_{D_r}}{<\psi>_{D_r}} \tag{21}$$

Similar expressions also stand for cross sections that are implicit in q_r (scattering and production).

At this point, the above equations suffer from no approximation except assumption (14). They however cannot be avoided if the dependence on the 3D flux ψ is to be dropped out in transverse leakage L_i, L_r and in the averaged cross section Σ_r.

III.B. Approximations for SFRs

This paper addresses the topic of cross sections averaging so geometrical domain D only needs to be a subdomain of the core suited for computation of representative weight functions (flux moments). In the following we therefore suppose that D is a radially reflected 3D pattern (a fuel assembly for instance).

In SFRs neutrons have quite large mean free paths (up to a few centimeters) and it is possible to assume that neutron fluxes are locally flat. We therefore consider no radial partitioning of domain D but only an axial splitting i.e. $D = \bigcup_i Z_i \times D_r$.

Under those circumstances, the zero net radial leakage boundary condition (radial reflection) over ∂D_r leads to

$$L_r = 0 \tag{22}$$

If we also neglect the radial dependence of leakage L_i and integrate equation (19) over D_r, we get

$$L_i = \frac{\mu}{A_{xy}}\int_{Z_i} dz\ \partial_z\psi_r = \frac{\mu}{A_{xy}}\psi_r|_{z_i-}^{z_i+} \tag{23}$$

with $A_{xy} = \int_{D_r} dxdy$ and $Z_i = [z_i-; z_i+]$.

Finally, assuming that the change in the radial flux shape is small along Z_i, cross section Σ_r can be averaged with 2D flux ψ_i instead of 3D flux ψ i.e.

$$\Sigma_{r,i} = \frac{< \Sigma\psi_i >_{D_r}}{< \psi_i >_{D_r}} \tag{24}$$

Most 2D/1D methods neglect the angular dependences in the homogenized cross sections and use a scalar flux weighting in the above equation. However, the preservation of anisotropic effects in transport calculations requires higher order methods as it was pointed out in Sec. II.B. In this paper, the flux moments weighting technique (i.e. equations (10), (11) and (12)) is used. Other solutions such as polar angle dependent cross sections [19] might also be found in the literature but their number is limited.

Introducing those approximations in the 2D/1D system, we find that equation (15) becomes a 2D equation for flux ψ_i with imposed external source L_i while equation (16) becomes a standard 1D eigenvalue problem for flux ψ_r with homogenized cross section Σ_r. They form the closed system of coupled 2D/1D equations.

III.C. Interest for cross sections collapsing

The 2D/1D system of equations defines a natural algorithm for producing effective cross sections that preserve 3D transport effects at a relatively low computational cost. A schematic view of this algorithm is presented in Figure 1. It reads:

1. Initialize leakage L_i
2. Compute 2D fluxes ψ_i with eq. (15)
3. Homogenize cross sections $\Sigma_{r,i}$ with eq. (24)
4. Compute 1D flux with eq. (16) and (22)
5. Compute axial leakage L_i with eq. (23)
6. Go back to point 2 until convergence
7. Compute effective cross sections

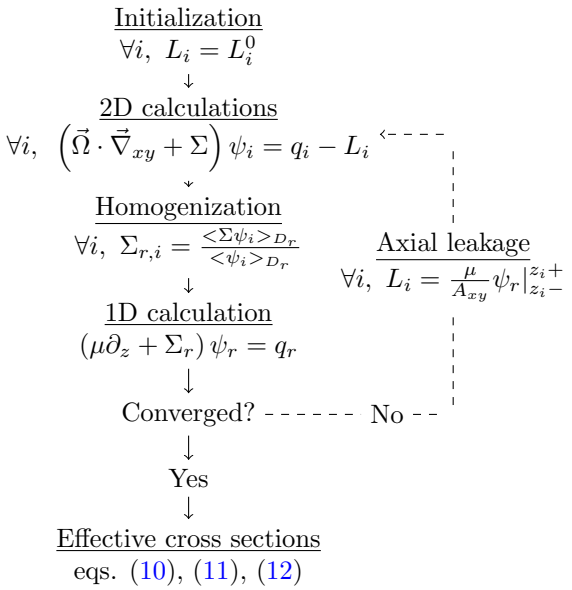

Fig. 1. 2D/1D algorithm for effective cross sections generation

Convergence of the algorithm can be checked on 2D or 1D fluxes, effective cross sections or, more simply, on the 1D eigenvalue. In Sec. IV, this latter test will be used.

The main interest of the 2D/1D equations for cross sections collapsing is the representation of the angular variable. In standard 2D patterns (lattice paradigm), high order angular modes of the flux are often close to zero because anti-symmetric modes with respect to the (xOy) plane do not exist and reflective boundary conditions also alter radial moments. As a consequence, $< \phi_{lm} >_i$ is close to 0 for $l > 0$ and equation (12) cannot be used to collapse high order cross sections. On the contrary, the 2D/1D framework involve full angular fluxes. So consistent flux moments can be used to collapse cross sections (if such moments exist in the 3D geometry).

Another interesting feature of the 2D/1D algorithm is that it naturally takes into account spectrum shifts along the (Oz) axis while it is not the case of standard 2D lattice calculations.

Moreover the algorithm provides a way to compute effective cross sections in media that have a low (or null) intrinsic neutron source (e.g. fertile blankets or shields) and avoids thus the construction of ad-hoc sources or cluster geometries.

Finally, the 2D/1D approximation avoids full 3D simulations and offers flexibility in two dimensional simulations that can be performed independently. In addition, axially non-conformal geometries can be treated without any restriction.

III.D. Practical implementation

The previous algorithm has been implemented in the APOLLO3® code to test its validity.

In their most general form, equations (15) and (16) involve 3D angular representations of fluxes ψ_i and ψ_r. However, the trajectory sweeping in standard 2D and 1D solvers is done accordingly to the symmetries present in the geometry. As a consequence some angular moments are automatically set to 0 and the 3D angular information is lost. So particular solvers are required.

III.D.1. 2D solver

A special version of the TDT MOC solver [20] was recently developed in APOLLO3® to solve the *heterogeneous B equations* in 2D geometries. Those equations come from the theory of neutron leakage in infinite lattices [21] and read

$$\left(\vec{\Omega}\cdot\vec{\nabla}+\Sigma+i\vec{B}\cdot\vec{\Omega}\right)\psi=q \tag{25}$$

The TDT-B solver sweeps polar angles in the full $[0;\pi]$ range so 3D angular representations are allowed for the flux. If the buckling vector $\vec{B}$ is set to 0, equation (25) is formally identical to equation (15) so the TDT-B solver can be used to solve the 2D equations.

III.D.2. 1D solver

When approximations of Sec. III.B are made, radial leakage are set to zero in equation (16). So the right hand side of the equation is not impacted by 3D angular effects. In addition, the *moments* weighting technique does not introduce particular angular dependences in the homogenized 1D cross sections. As a result, a standard 1D solver can be used. In this paper, the short characteristics IDT solver [22] of APOLLO3® is chosen.

III.D.3. 2D/1D coupling

Axial leakage L_i are computed from 1D interface angular fluxes with equation (23). They are then projected over Legendre polynomials P_l and identified to rotationally (Oz)-invariant angular

moments for 2D calculations

$$L_{i,lm} = \begin{cases} \dfrac{1}{A_{xy}} \displaystyle\int_{\mu=-1}^{+1} d\mu \; P_l(\mu)\mu \left[\psi_r(z,\mu)\right]_{z_i-}^{z_i+} & \text{if } m = 0 \\ 0 & \text{otherwise} \end{cases} \tag{26}$$

III.D.4. Fix-up for negative sources

There is no guarantee that the total source in the right hand side of equation (15) is positive. As a result, instabilities and even negative fluxes can be found when axial leakage are strong enough. In reference [17], this issue is addressed with *transverse leakage splitting* and the negative source is turned into an additional absorption term.

In this work however, it has been chosen to avoid intrusions in flux solvers so the positiveness of $q_i - L_i$ is never tested. Stability of the algorithm is nevertheless guaranteed by neglecting physical leakage i.e.

$$L_i = 0 \text{ when } -L_i < 0 \tag{27}$$

In sub-critical and non multiplicative 2D layers $Z_i \times D_r$ (shields or fertile blankets), approximation (27) does not affect the stability of the algorithm because the existence of a neutron source $q_i - L_i$ is ensured for all energy groups: $-L_i > 0$ at high energies (arrival of high energy neutrons from main fissile zones) and $q_i > 0$ at low energies (down-scattering effect).

For over-critical 2D layers (fuel) on the contrary, approximation (27) creates the condition of an over-critical pattern with positive external source. In such a situation, no solution of the transport equation exists so any iterative resolution of equation (15) is condemned to diverge. The physical interpretation is that leakage cannot be neglected in over-critical layers. If positiveness of the source $q_i - L_i$ does not want to be tested, an artifact must then be used to replace real leakage by fictitious ones. The arbitrary choice we made in this paper is to use the heterogeneous B equations (25) to account for leakage out of 2D overcritical layers. In other words, real leakage are replaced by a buckling vector $\vec{B}$ in such patterns. Because $\vec{B}$ accounts for axial leakage, we choose its orientation along (Oz). Its amplitude B^2 is also adjusted to ensure $k(B^2) = 1$. If those choices are purely arbitrary, they considerably simplify the 2D/1D algorithm since they imply that overcritical layers can be calculated once and for all at the beginning of the iterative strategy.

Reflections are currently under consideration to mitigate those rather crude approximations. Despite all, we shall see in the next section that quite good results could be obtained.

IV. NUMERICAL RESULTS FOR A SFR ASSEMBLY CALCULATION

IV.A. Problem description

The benchmark chosen for analysis of the 2D/1D algorithm is a hexagonal SFR fuel assembly representative of the ASTRID core. The geometry shows strong axial heterogeneities (CFV design) so axial flux gradients are expected.

The axial layout of the core is depicted in Figure 2.a. C1 stands for fissile (U,Pu)O_2 material while FCA is for fertile UO_2 media. PLN and PNS are French acronyms for sodium plenum and axial neutronic protection respectively. Radial mesh of the fuel pins lattice is presented in Figure 2.b while plenum is shown in Figure 2.c. Dimensions and compositions of the benchmark are available in reference [2] except for the axial protection (Figure 2.d) that was not modeled is that former work. The latter is composed of a lower plug and a 57.5 cm height column of B_4C absorber material (7.5 cm 90% ^{10}B enriched + 50 cm natural boron).

The axial partition of domain D for the 2D/1D algorithm follows the axial layout of the assembly leading to thirteen 2D layers (TDT calculations). In IDT 1D calculations, the axial mesh is refined to ensure a converged flux solution (sub-plane scheme). Taking advantage of the algorithm flexibility, all radial heterogeneities are explicitly described in 2D layers.

Nuclear data are taken from the JEFF-3.1.1 evaluation and prepared into a 1968 group energy structure using the dedicated GALILEE processing tool [23]. A $P3$ angular order is chosen for the scattering kernel.

Before any flux calculation, cross sections are self-shielded over the exact 2D geometries using the Tone method of APOLLO3®, which has proven to give very good results for SFR calculations and even comparable with reference subgroup methods [2, 24].

Results of the 2D/1D algorithm are compared to reference Monte Carlo simulations that have been performed with the TRIPOLI4® code. A very large number of neutron histories have been sampled over the exact 3D geometry description and with continuous representations of the angle and energy variables. To ensure consistency of nuclear data, mathematical probability tables have been used in the unresolved resonances region.

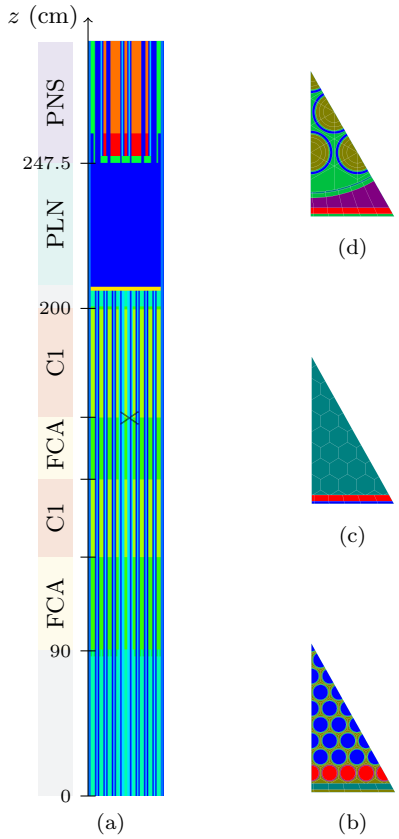

Fig. 2. ASTRID internal fuel assembly: (a) axial layout, (b) fuel pins mesh, (c) sodium plenum mesh, (d) axial protection mesh

IV.B. Algorithm validation

Before considering the generation of effective cross sections, the behavior of the 2D/1D algorithm itself is tested. In particular, convergence is checked on the 1D eigenvalue k and the influence of initialization is discussed.

IV.B.1. Convergence

Table I shows the reactivity error towards reference value

$$\Delta\rho = 10^5 \left(\frac{1}{k_{\text{ref}}} - \frac{1}{k} \right) \tag{28}$$

as a function of the number of iterations in the 2D/1D algorithm. An iteration, identified in the following with superscript n, is defined as a complete loop in Figure 1 starting from 2D calculations.

For overcritical layers we recall that the B equations (25) are solved once and for all in the first iteration. The B *leakage rate* is used as an initialization source $L_i^{(0)}$ for all other planes (FCA, PLN...). 1D cross sections $\Sigma_{r,i}^{(n)}$ are homogenized with 2D flux moments i.e. with equations (10), (11) and (12).

Reference	$k = 1.08183 \pm 1$ pcm		
2D/1D	Iteration n°		
	1	2	3
$\Delta\rho$ (pcm)	+164	+69	+69

TABLE I
Convergence of the 1D eigenvalue in 2D/1D algorithm

We see that the algorithm converges quickly and that the reactivity discrepancy towards reference Monte Carlo results is limited ($\Delta\rho = 69$ pcm). More precisely, we observe that only two iterations are necessary before matching convergence: $\Delta\rho^{(3)} = \Delta\rho^{(2)}$. The interpretation is that 1D homogenized cross sections $\Sigma_{r,i}$ are in fact not affected by small variations in the sources L_i that are used for computation of 2D homogenization fluxes ψ_i. In other words, the first 1D calculation contains enough information to compute *accurate-for-homogenization* sources L_i.

Furthermore, it has been observed that non-multiplicative and sub-critical layers flux calculations are not even necessary in first iteration. In fact, cross sections $\Sigma_{r,i}^{(1)}$ can be homogenized with a constant flux shape ($\psi_i^{(1)} = 1$) without impacting the final results. This fact can be formally checked in the second line of Table II that shows the reactivity error when only overcritical layers are computed in iteration 1.

Computed in	Iteration n°		
iteration 1	1	2	3
All layers	+164	+69	+69
Only over-critical	-6	+69	+69

TABLE II
Influence of initialization in 2D calculations

IV.B.2. Influence of buckling normalization for over-critical layers

As mentioned in Sec. III.D, the 2D/1D equations are not used for overcritical layers but equation (25) is solved at the beginning of the iterative process. The buckling $\vec{B}$ is directed along the (Oz) axis and its modulus $|\vec{B}|$ adjusted so that $k(B^2) = 1$.

However, this choice is purely arbitrary and it could as well be decided to adjust more subtly $|\vec{B}|$, for instance scaling $k(B^2)$ to the current iteration 1D eigenvalue . This *dynamic scaling* has been tested but it was found that its impact on the final result was negligible (less than 5 pcm) compared to the increased number of 2D flux calculations it required.

IV.B.3. Optimization

With the above considerations, a significant number of flux calculations can be avoided without impacting accuracy of the final results. In fact, we are able to define an algorithm in which only one flux calculation is performed for each 2D layer. It reads:

1. Solve B equations (25) for overcritical layers imposing $k(B^2) = 1$
2. Initialize $\psi_i = 1$ for all other 2D layers
3. Homogenize cross sections $\Sigma_{r,i}$ with eq. (24)
4. Compute 1D flux with eq. (16) and (22)
5. Compute axial leakage L_i with eq. (23)
6. Compute 2D fluxes ψ_i with eq. (15)
7. Compute effective cross sections

In this optimized version of the 2D/1D algorithm, 2D fluxes ψ_i are used to weight cross sections in point 7. Equations (10) (11) and (12) are used.

IV.C. Assembly calculation with effective cross sections

In this section, the optimized algorithm is used to produce effective cross sections. The 1968 group energy structure is condensed into 33 groups and homogenization is performed over each axial layer Z_i. A library with thirteen sets of 33 group homogenized cross sections is therefore built.

With this library, we are capable of defining a simplified model of the initial benchmark over which the transport equation (1) can be solved. This model is chosen to stress the 2D/1D averaged cross sections against reference continuous energy heterogeneous 3D Monte Carlo simulations.

The S_N MINARET solver [25] of APOLLO3® is used to solve the transport equation over the simplified fuel assembly model. Fine spatial and angular discretizations (2.5 cm axial mesh and 144 angle directions) ensure that the flux is converged.

Results for eigenvalues and fission rate distributions, in nominal and voided conditions, are presented in Table III and Figure 3. Equation (28) is used for the reactivity discrepancy between APOLLO3® and TRIPOLI4® .

To show the need for high order angular moments, results with (scalar) flux volume weighted cross sections are also reported in the second line of Table III. This is done using the same 2D/1D flux distribution but replacing ϕ_{lm} by ϕ_{00} in equation (12) to obtain the standard flux volume weighting formula.

	Nominal	Voided	Void worth
Reference	$k \pm 10^5 \delta k$	$k \pm 10^5 \delta k$	$\Delta\rho_{\mathrm{Na}}$ (pcm)
Monte Carlo	1.08183 ± 1	1.06399 ± 1	-1550 ± 2
2D/1D	$\Delta\rho$ (pcm)	$\Delta\rho$ (pcm)	$\Delta(\Delta\rho_{\mathrm{Na}})$
ϕ_{lm}	-58	-39	+19
ϕ_{00}	+288	+625	+337

TABLE III
Results for fuel assembly calculation in nominal and voided situations. Reference eigenvalue / sodium void worth and reactivity discrepancy (towards reference) using 33 group homogenized cross sections generated with 2D/1D algorithm. ϕ_{lm} (resp. ϕ_{00}) stands for flux moments (resp. scalar flux) averaged XS.

It is seen that very good performances are obtained with 2D/1D cross sections when high order angular modes of the flux (moments ϕ_{lm}) are used. The results reproduce the Monte Carlo ones within a 60 pcm range for reactivity and within a 1% relative discrepancy for the fission rate distribution. A slightly larger error is found in coolant voided fertile material but in such regions the fission rate is relatively low.

As for the 127 pcm reactivity difference that is found between the 33 group MINARET calculation ($\Delta\rho = -58$ pcm) and the 1968 group IDT results ($\Delta\rho = +69$ pcm in Sec. IV.B), it mainly accounts for the reduction in the number of energy groups and, to a lesser extent, for differences in flux solvers.

In the other hand, we observe that very large errors arise when only the isotropic component of the flux (ϕ_{00}) is used to weight cross sections. In particular, a +625 pcm reactivity discrepancy is found in voided conditions leading to a +337 pcm error in the sodium void worth. This last

value is comparable to typical SFR delayed neutron fractions $\beta \approx 360$ pcm and thus far from being compatible with safety requirements.

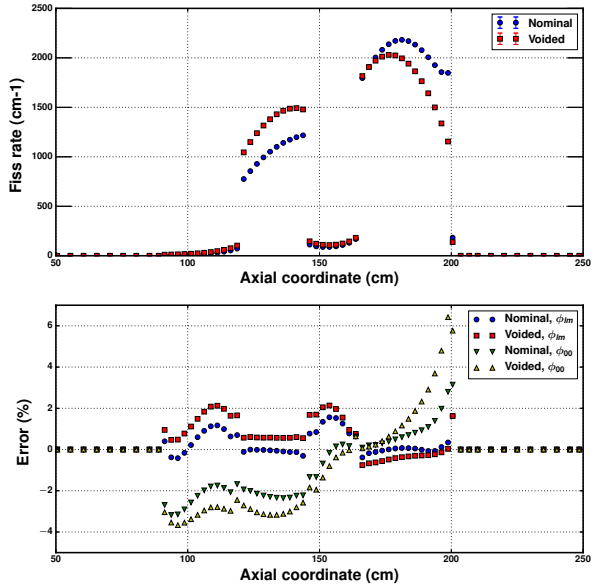

Fig. 3. Fission rate distribution (top) and relative error with reference results using 33 group homogenized cross sections generated with 2D/1D algorithm (bottom). ϕ_{lm} (resp. ϕ_{00}) stands for flux moments (resp. scalar flux) averaged XS.

Therefore, the conclusion is that neutron transport physics in SFRs and even CFV-like designs can be accurately modeled with 33 group homogenized cross sections. Consistent information is however required for high angular order data else results strongly deteriorate.

Looking at the computational efficiency of the 2D/1D algorithm, a gain of a factor 5 to 10 was found on both calculation time and memory requirements compared to full 3D MOC simulations (with axial polynomial expansion [3]). We however point out that results are not fully comparable because acceleration methods for the TDT-B solver are still under development, making it possible to expect a greater gain in the time needed to solve the 2D/1D equations. All calculations have been run with OMP parallelism on a 4 threads cluster node with Intel(R) Xeon(R) CPU E5-2630 v4 @ 2.20 GHz.

V. CONCLUSION

This paper presents an efficient algorithm to produce effective cross sections for SFR whole core transport calculations.

The 2D/1D method is used to approximate the 3D Boltzmann transport equation while preserving consistent representation of angular fluxes. The stability of the algorithm is numerically checked and the accuracy of the effective cross sections verified against reference Monte Carlo simulations.

The benchmark chosen for application is a radially reflected fuel assembly representative of the ASTRID CFV core. It is shown that very good accuracy is achieved with the 33 group homogenized 2D/1D cross sections, both in nominal and voided situations. It is also proven that high order angular information must absolutely by stored in the effective cross sections.

The algorithm presented in this paper is subject to two main sources of errors that should be commented. The first one is the flat flux approximation that is used to compute transverse leakage and homogenize 2D cross sections. If consequences of this assumption are likely to be limited in SFRs where neutrons have large mean free paths, it should be used with caution for other applications such as PWR calculations.

The second source of error is the fix-up used for negative sources. Because it replaces physical leakage by empirical ones and even neglects them in sub-critical layers, it breaks the neutronics balance in 2D calculations. Further work shall investigate quantitatively the impact of this approximation on effective cross sections to state whether it should be mitigated or not (for instance with a transverse leakage splitting technique).

Finally, undergoing work tends at confirming that the 2D/1D algorithm produces accurate effective cross sections for realistic industrial applications i.e. full core calculations with radial reflector, control rods... As for reactor cycle calculations, the algorithm provides a natural way to parametrize cross sections with realistic local burn-ups: the 3D fuel assembly power (thermohydraulics data) can be used to normalize 1D fluxes and run the isotopic depletion calculations for each axial evolving layer. Future work shall also investigate this possibility.

ACKNOWLEDGMENTS

The authors acknowledge the CEA of Cadarache for funding this work and AREVA and EDF for their long term support. They also thank the APOLLO3® development team for their effort in developing the code. One of the authors (B.F.) would like to address many thanks to S. Santandrea and E. Masiello for their great help while developing the methods presented in this paper.

REFERENCES

[1] R. Sanchez, "Prospects in deterministic three-dimensional whole-core transport calculations," *Nuclear Engineering and Technology*, **44**, *2*, 113 (2012).

[2] B. Faure, P. Archier, J.-F. Vidal, J. M. Palau, and L. Buiron, "Neutronic calculation of an axially heterogeneous ASTRID fuel assembly with APOLLO3®: Analysis of biases and foreseen improvements," *Annals of Nuclear Energy*, **115**, 88 (2018).

[3] S. Santandrea, L. Graziano, and D. Sciannandrone, "Accelerated polynomial axial expansions for full 3D neutron transport MOC in the APOLLO3 code system as applied to the ASTRID fast breeder reactor," *Annals of Nuclear Energy*, **113**, 194 (2018).

[4] N. Z. Cho, G. S. Lee, and C. J. Park, "A fusion technique of 2D/1D methods for three-dimensional whole-core transport calculations," *Proc. Korean Nuclear Society* (2002).

[5] D. Schneider, F. Dolci, F. Gabriel, J. Palau, M. Guillo, and B. Pothet, "APOLLO3: CEA/DEN deterministic multi-purpose code for reactor physics analysis," *Proc. Int. Conf. PHYSOR 2016 - Unifying Theory and Experiments in the 21st Century*, American Nuclear Society, Sun Valley, Idaho, United States (2016).

[6] J. Vidal, P. Archier, A. Calloo, P. Jacquet, J. Tommasi, and R. Le Tellier, "An improved energy-collapsing method for core-reflector modelization in SFR core calculations using the PARIS platform," *PHYSOR 2012 - Advances in Reactor Physics - Linking Research, Industry and Education*, American Nuclear Society (2012).

[7] R. Sanchez, "Assembly homogenization techniques for core calculations," *Progress in Nuclear Energy*, **51**, *1*, 14 (2009).

[8] A. Hébert and G. Mathonnire, "Development of a third-generation superhomogeneisation method for the homogenization of a pressurized water reactor assembly," *Nuclear Science and Engineering*, **115**, *2*, 129 (1993).

[9] K. S. Smith, "Assembly homogenization techniques for light water reactor analysis," *Progress in Nuclear Energy*, **17**, *3*, 303 (1986).

[10] F. Rahnema, S. Douglass, and B. Forget, "Generalized energy condensation theory," *Nuclear Science and Engineering*, **160**, *1*, 41 (2008).

[11] S. Douglass and F. Rahnema, "Consistent generalized energy condensation theory," *Annals of Nuclear Energy*, **40**, *1*, 200 (2012).

[12] J.-F. Vidal, P. Archier, B. Faure, V. Jouault, J.-M. Palau, V. Pascal, G. Rimpault, F. Auffret, L. Graziano, E. Masiello et al., "APOLLO3 Homogenization Techniques for Transport Core Calculations - Application to the ASTRID CFV Core," *Nuclear Engineering and Technology* (2017).

[13] J.-Y. Cho, K.-S. Kim, C.-C. Lee, S.-Q. Zee, and H.-G. Joo, "Axial SPN and radial MOC coupled whole core transport calculation," *Journal of nuclear science and technology*, **44**, *9*, 1156 (2007).

[14] Y. S. Ban, E. Masiello, R. Lenain, H. G. Joo, and R. Sanchez, "Code-to-code comparisons on spatial solution capabilities and performances between nTRACER and the standalone IDT solver of APOLLO3," *Annals of Nuclear Energy*, **115**, 573 (2018).

[15] X. Tang, Q. Li, X. Chai, X. Tu, W. Wu, and K. Wang, "Efficient procedure for radial MOC and axial SN coupled 3D neutron transport calculation," *Proc. Int. Conf. on Mathematics and Computational Methods Applied to Nuclear Science and Engineering (M&C2017)*, American Nuclear Society (2017).

[16] B. W. Kelley and E. W. Larsen, "A consistent 2D/1D approximation to the 3D neutron transport equation," *Nuclear Engineering and Design*, **295**, 598 (2015).

[17] B. Collins, S. Stimpson, B. W. Kelley, M. T. Young, B. Kochunas, A. Graham, E. W. Larsen, T. Downar, and A. Godfrey, "Stability and accuracy of 3D neutron transport simulations using the 2D/1D method in MPACT," *Journal of Computational Physics*, **326**, 612 (2016).

[18] G. S. Lee and N. Z. Cho, "2D/1D fusion method solutions of the three-dimensional transport OECD benchmark problem C5G7 MOX," *Progress in Nuclear Energy*, **48**, *5*, 410 (2006).

[19] M. Jarret, B. Kochunas, E. Larsen, and D. T, "Characterization of 2D/1D accuracy in MPACT," *Proc. Int. Conf. on Mathematics and Computational Methods Applied to Nuclear Science and Engineering (M&C2017)*, American Nuclear Society (2017).

[20] S. Santandrea, "An Integral Multidomain DPN Operator as Acceleration Tool for the Method of Characteristics in Unstructured Meshes," *Nuclear Science and Engineering*, **155**, *2*, 223 (2007).

[21] V. Deniz, "The Theory of Neutron Leakage in Reactor Lattices," R. Yonen (Editor), *CRC Handbook of Nuclear Reactor Calculations*, vol. II, 409 – 508, CRC Press.

[22] I. Zmijarevic, "IDT solution to the 3D transport benchmark over a range in parameter space," (2008).

[23] M. Coste-Delclaux, "GALILEE: A nuclear data processing system for transport, depletion and shielding codes," *Proc. Int. Conf. PHYSOR 2008 - Nuclear Power: A Sustainable Resource*, American Nuclear Society (2008).

[24] L. Mao and I. Zmijarevic, "A new Tone's method in APOLLO3® and its application to fast and thermal reactor calculations," *Nuclear Engineering and Technology*, **49**, *6*, 1269 (2017).

[25] J. Moller, J. Lautard, and D. Schneider, "MINARET, a deterministic neutron transport solver for nuclear core calculations," *Proc. Int. Conf. on Mathematics and Computational Methods Applied to Nuclear Science and Engineering (M&C2011)*, American Nuclear Society (2011).